

Lawrence Berkeley National Laboratory

LBL Publications

Title

Inclusive Charged Hadron and K^0 Production in Two-Photon Interactions

Permalink

<https://escholarship.org/uc/item/7b20k879>

Authors

Cords, D.
Boyer, J.
Butler, F.
et al.

Publication Date

1992-08-01

DISCLAIMER

This document was prepared as an account of work sponsored by the United States Government. While this document is believed to contain correct information, neither the United States Government nor any agency thereof, nor the Regents of the University of California, nor any of their employees, makes any warranty, express or implied, or assumes any legal responsibility for the accuracy, completeness, or usefulness of any information, apparatus, product, or process disclosed, or represents that its use would not infringe privately owned rights. Reference herein to any specific commercial product, process, or service by its trade name, trademark, manufacturer, or otherwise, does not necessarily constitute or imply its endorsement, recommendation, or favoring by the United States Government or any agency thereof, or the Regents of the University of California. The views and opinions of authors expressed herein do not necessarily state or reflect those of the United States Government or any agency thereof or the Regents of the University of California.

SLAC-PUB-5901
LBL-32903
August 1992
(T/E)

**Inclusive Charged Hadron and K^0 Production
in Two-Photon Interactions***

D. Cords, J. Boyer, F. Butler, G. Gidal,
G. S. Abrams, D. Amidei, A. R. Baden, T. Barklow, A. M. Boyarski, P. R. Burchat,
D. L. Burke, J. M. Dorfan, G. J. Feldman, L. Gladney,
M. S. Gold, G. Goldhaber, J. Haggerty, G. Hanson, K. Hayes,
D. Herrup, R. J. Hollebeek, W. R. Innes, J. A. Jaros, I. Juricic, J. A. Kadyk,
D. Karlen, A. J. Lankford, R. R. Larsen, B. W. LeClaire, M. E. Levi, N. S. Lockyer,
V. Lüth, M. E. Nelson, R. A. Ong, M. L. Perl,
K. Riles, P. C. Rowson, T. Schaad, H. Schellman, W. B. Schmidke,
G. H. Trilling, D. R. Wood, and J. M. Yelton

*Lawrence Berkeley Laboratory and Department of Physics
University of California, Berkeley, California 94720*

*Stanford Linear Accelerator Center
Stanford University, Stanford, California 94305*

*Department of Physics
Harvard University, Cambridge, Massachusetts 02138*

Abstract

The inclusive transverse momentum distributions of charged hadrons and K^0 's produced in tagged photon-photon collisions, are measured and compared to model calculations up to a p_T of 5 GeV/c. The relative abundance of K^0 's favor the inclusion of charm.

* This work was supported in part by the Department of Energy, contracts DE-AC03-76SF00515 and DE-AC03-76SF00098.

A process analogous to quark pair production in e^+e^- annihilation is the hard-scattering quark exchange process in $\gamma\gamma$ interactions. This hard-scattering process is expected to dominate ¹⁾ the cross section at high transverse momenta of the produced quarks. Experimentally, one has looked for this process in two-jet ²⁾ as well as inclusive particle ^{3,4)} production and has found a relatively low p_T onset of hard scattering in $\gamma\gamma$ interactions. This report examines the issue in more detail (high statistics) for charged particle inclusive production and checks if the heavier flavors display a similar behavior in inclusive K^0 production.

The results⁵⁾ are based on an integrated luminosity of 220 pb⁻¹ obtained with the Mark II detector at PEP operating at $E_{CM} = 29$ GeV. The major features of the Mark II detector have been described elsewhere⁶⁾. The combined tracking information from the central drift chamber and the vertex drift chamber in a 2.3 kG magnetic field provided a momentum resolution of $(\sigma(p_T)/p_T)^2 = (0.025)^2 + (0.011p_T)^2$ (p_T in GeV/c). The small angle tagging system (SAT) measures electrons scattered between 21 and 83 mrad from the beam axis. It consists of three layers of drift chambers with a spatial resolution of 300 μ m in the xy plane, followed by three layers of acceptance defining scintillator and 18 alternating layers of 1/4 inch lead and 1/2 inch scintillator. The energy resolution achieved for electrons is $\sigma/E = 15.5\%/\sqrt{E}$.

We detect some 60,000 events tagged by an electron in the SAT corresponding to a Q^2 interval between 0.075 and 1.00 GeV². Since we do not observe the entire final state, the transverse momentum of hadrons, p_T , is calculated in the usual manner, with respect to the e^+e^- beam axis. To eliminate the large QED background we accept only events with 3 or more charged tracks observed (in addition to the tagging electron). Events having identified leptons are removed using the Liquid Argon Calorimeter and the muon chambers. To minimize the beam-gas interaction background we also eliminate events with protons or deuterons identified by their time of flight. The background from $e^+e^- \rightarrow e^+e^- \tau^+\tau^-$ is subtracted using the Monte Carlo simulation of this process. The residual background from beam-gas interactions is simulated with events produced along the beam-line outside the in-

teraction region. Both these backgrounds vary between 5% and 10% with p_T and are subtracted from the data. Taking advantage of the precision vertex chamber, a vertex finding program (VFINDP) is used to find K^0 's which decay at least 2.5 mm from the primary vertex. After several quality cuts, tracks are combined into charge zero pairs and the points of intersection are calculated. Of the two possible crossing points in the x-y plane, the program chooses the one which gives a positive decay length and is nearest to the interaction point. The track momenta are corrected for energy loss in the material traversed and the tracks are constrained to pass through a single point in space. The $\pi^+\pi^-$ pair mass distribution shows a clear K^0 peak with a resolution of $\sigma = 7$ MeV and an estimated background of less than 8%. We select events with masses in an interval ± 20 MeV about the actual K^0 mass.

A Two-Photon Monte Carlo program⁷⁾ is used to simulate the hard scattering quark exchange process $e^+e^- \rightarrow e^+e^- q\bar{q}$, or for short $\gamma\gamma \rightarrow q\bar{q}$. It incorporates transverse-transverse as well as transverse-longitudinal $\gamma\gamma$ luminosity functions⁸⁾, a summation over the four quark flavors u,d,s,c, and the subsequent fragmentation of the quarks according to the LUND scheme⁹⁾. The ambiguities and variations in jet definitions at these low energies make it preferable to directly measure single particle inclusive cross sections. For this analysis we have ignored the Vector Dominance Model (VDM) contributions. The rather steep fall-off with p_T makes this a negligible contribution above $p_T = 2$ GeV/c¹²⁾. The quark fragmentation parameters are taken as the set of values which best describe the e^+e^- annihilation data at 29 GeV, and no attempt has been made to optimize the parameters for the lower two-photon energies. Since the quark flavors enter with the fourth power of their charges, the most important contributions come from the u and c quarks once the available two-photon energy exceeds the respective quark pair thresholds. These Monte Carlo calculations describe the gross features of the data and are used to obtain the detection efficiencies for the various particle species. The efficiencies rise with p_T and reach about 17% for charged hadrons and 3.3% for K^0 's at $p_T = 2$ GeV. They include the trigger simulation and the correct threshold

behavior for charm production.

As first pointed out by TASSO³⁾ the p_T distribution of single charged hadrons does not follow a simple exponential fall-off but flattens out for p_T values above 1 GeV. Similar to the TASSO procedure, the Mark II analysis uses single tag data with Q^2 values around 0.5 GeV², but with its higher statistics Mark II can extend the sensitive range in p_T from 3 to 5 GeV. In Fig. 1 the inclusive charged hadron cross section multiplied by p_T^3 is plotted as a function of p_T . After the initial steep drop the data points are consistent with being constant for p_T values above 3 GeV. This flat part of the distribution translates into a p_T^{-4} behaviour for $d\sigma/dp_T^2$ and is an indication of the underlying structure of a scale-invariant point-like process, the simplest manifestation of which is the hard scattering quark exchange process $\gamma\gamma \rightarrow q\bar{q}$. Several authors have calculated $d\sigma/dp_T^2$ for this process in the quark parton model, and it has been shown earlier¹⁰⁾ that any p_T dependence due to quark hadronization is small compared to the p_T^{-4} power law as long as one stays away from kinematic boundaries. Therefore, we can expect for our analysis a somewhat modified p_T^{-4} behaviour for the inclusive particle spectrum, if the scaled transverse momentum $x_T = p_T/p_{beam}$ is small compared to 1. For the data in Fig. 1 x_T is in the range between 0.07 and 0.34.

Nevertheless, the fragmentation introduces some uncertainty in the comparison of our data with the underlying hard scattering process. It is therefore more appropriate to compare the data with a Monte Carlo simulation of the process $\gamma\gamma \rightarrow q\bar{q}$, for which the fragmentation parameters have been adjusted in the clean environment of e^+e^- annihilation as mentioned above. The ratio of the measured and calculated inclusive cross-sections is shown in Fig. 2. The enhancement below 2 GeV is mainly due to vector dominance processes, which are not included in the Monte Carlo. The remarkable feature is that the ratio is approximately constant and compatible with 1 for p_T values above about 2 GeV. This means that the hard scattering process accounts for most of the high p_T hadron production. Contributions from higher order hard scattering processes with 3 or 4 quarks and/or gluons can be important for moderate p_T values and for $Q^2 = 0$. However, it has

been shown experimentally¹¹⁾ that any excess over the $\gamma\gamma \rightarrow q\bar{q}$ process decreases dramatically as Q^2 increases. In addition, most detectors are less sensitive to these higher order processes, since the additional spectator quarks and/or gluons are produced close to the beam direction.

With its ability to identify K^0 's over a wide momentum range the Mark II detector can be used to look for the onset of charm production, because due to its charge, strange-quark production is expected to be suppressed by a factor of 16 with respect to charm quarks. With the same absolute normalization as above, the ratio of inclusive K^0 's from data and Monte Carlo is shown in Fig. 3 for p_T values up to 3 GeV. Although the errors are much larger here, the data are consistent with the same general features observed for charged hadron production. The ratio of K^0 's to charged hadrons increases to about 30% at the highest p_T values as shown in Fig. 4. From the Monte Carlo simulations with and without charm one can ascertain that the charm quarks are responsible for about half the K^0 production (difference between solid and dashed lines) at high p_T . Combining the highest p_T bins we find $R(p_T > 1.6 \text{ GeV}/c) = 0.30 \pm .08$. This can be compared with Monte Carlo values of 0.32 and 0.16 with and without the charm-quark contributions.

In an attempt to resolve the discrepancy between the Born term calculations and the untagged TASSO inclusive particle data⁴⁾, Aurenche et al. have performed model calculations¹²⁾ including higher order QCD terms and generalized vector dominance model contributions (motivated by photo-production data). The authors have subsequently expanded their calculations to include charm production and to extrapolate to the Mark II tagging range¹³⁾. We have folded their single charged hadron inclusive spectrum with the p_T resolution expected for the Mark II detector. As seen in Fig. 5 the data points lie systematically above the predictions of Aurenche et al. for p_T values larger than 1.5 GeV. However, the single-tag TASSO data³⁾ (in a similar Q^2 range as Mark II) show an even higher hadronic cross section. To be sure that the high p_T tail is not caused by the second final state electron scattering at large angles, we removed all events with electron candidates in the end caps or central detector. From Monte Carlo simulations we

expect at most 5 electrons with p_T above 2 GeV to go undetected in regions not properly covered by shower counters. The discrepancy between the model calculations and the Mark II data may be partially due to various effects: The tagging efficiency is only taken into account for an average Q^2 whereas there exists a moderate Q^2 dependence. The fragmentation may lead to uncertainties and is probably best handled with Monte Carlo methods. Analytic model calculations usually contain a number of approximations which may very well describe the overall features of a process but may lead to discrepancies in kinematic areas where the relative contributions have dropped by several orders of magnitude - as is the case for the high p_T tail discussed above. The model calculations have also not included multijet processes, for which there is recent experimental evidence at TRISTAN¹⁵⁾ confirming earlier indications at PEP¹⁶⁾ and PETRA^{11,14)}. However, the model calculations discussed here and our simple minded Monte Carlo simulations seem to describe different aspects (kinematic regions) of the data quite well.

In summary, we extend the investigation of inclusive charged hadron production to 5 GeV in p_T and find evidence for the hard scattering process $\gamma\gamma \rightarrow q\bar{q}$ in the p_T range from 3 to 5 GeV. With the first observation of inclusive K^0 production up to 3 GeV in p_T , we see the enhanced production expected from charm at high p_T values.

References

- 1) S.M. Berman, J.D. Bjorken, J.B. Kogut, Phys. Rev. **D4**, 3388(1971)
- 2) W. Bartel et al., Phys. Lett. **107B**, 163(1981); C. Berger et al., Z. Phys. **C33**, 351(1987)
- 3) R. Brandelik et al., Phys. Lett. **107B**, 290(1981)
- 4) M. Althoff et al., Phys. Lett. **138B**, 219(1984)
- 5) A preliminary report of these data was given in the proceedings of the VIIIth International Workshop on Photon-Photon Collisions, Shoresh, Jerusalem, Israel, April 1988 (World Scientific, Ed. U. Karshon)

- 6) R. Schindler et al., Phys. Rev. **D24**, 78(1981)
- 7) P. Bhattacharya et al., Phys. Rev. **D15**, 3267(1977); J. Smith et al., Phys. Rev **D15**, 3280(1977)
- 8) V.M. Budnev, I.F. Ginzburg, G.V. Meledin, and V.G. Serbo, Phys. Rep. **15**, 181(1975)
- 9) B. Anderson et al., Phys. Rep. **97**, 31(1983)
- 10) S. Brodsky et al., Phys. Rev **D19**, 1418(1979); K. Kajantie and R. Ratio, Nucl. Phys. **B159**, 528(1979)
- 11) C. Berger et al., Z. Phys. **C26**, 191(1984)
- 12) P. Aurenche, A. Douiri, R. Baier, M. Fontannez, D. Schiff, Z. Phys. **C29**, 423(1985)
- 13) P. Aurenche, R. Baier, M. Fontannez, D. Schiff, private communication
- 14) H.-J. Behrend et al., Z. Phys. **C51**, 365(1991)
- 15) R. Tanaka et al., Phys. Lett. **B277**, 215(1992)
- 16) H. Aihara et al., Phys. Rev. **41D**, 2667(1990)

FigureCaptions

Fig. 1: Differential cross section $p_T^3 d\sigma/dp_T$ as a function of the charged hadron transverse momenta p_T for single tagged events with $0.075 < Q^2 < 1.0 \text{ GeV}^2$. The dashed line represents a p_T^{-4} fall-off in $d\sigma/dp_T^2$.

Fig. 2: Inclusive charged hadron cross section ratio of experimental data to Monte Carlo $\gamma\gamma \rightarrow q\bar{q}$ events as a function of p_T ($0.075 < Q^2 < 1.0 \text{ GeV}^2$).

Fig. 3: Inclusive K^0 cross section ratio of experimental data to Monte Carlo $\gamma\gamma \rightarrow q\bar{q}$ events as a function of p_T ($0.075 < Q^2 < 1.0 \text{ GeV}^2$).

Fig. 4: Ratio of K^0 to charged hadron production as a function of p_T ($0.075 < Q^2 < 1.0 \text{ GeV}^2$). The full/dashed histograms are for Monte Carlo $\gamma\gamma \rightarrow q\bar{q}$ events with/without charm.

Fig. 5: Differential cross section $d\sigma/dp_T$ as a function of the charged hadron transverse momenta p_T ($0.075 < Q^2 < 1.0 \text{ GeV}^2$). The solid line is an analytic calculation by Aurenche et al.^{11,12}. The dashed line is a best fit to the data from TASSO³) and the dash-dotted lines an approximate 1 *sigma* contour around the data.

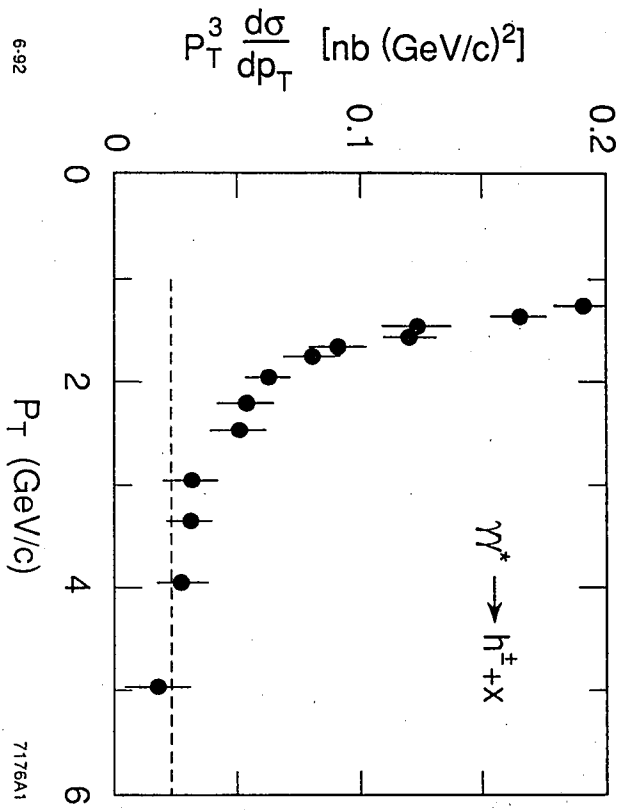


Fig. 1

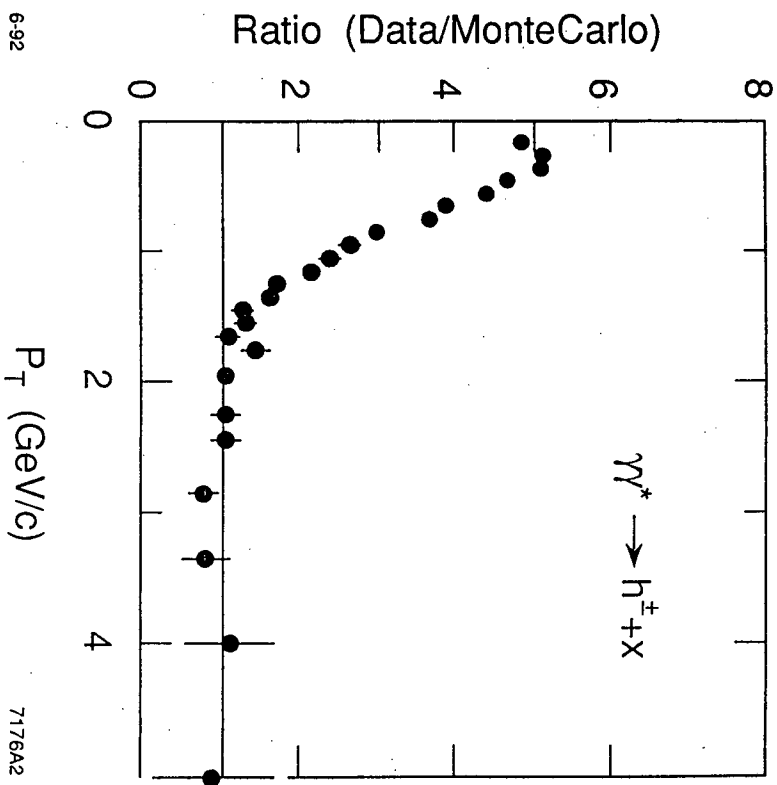


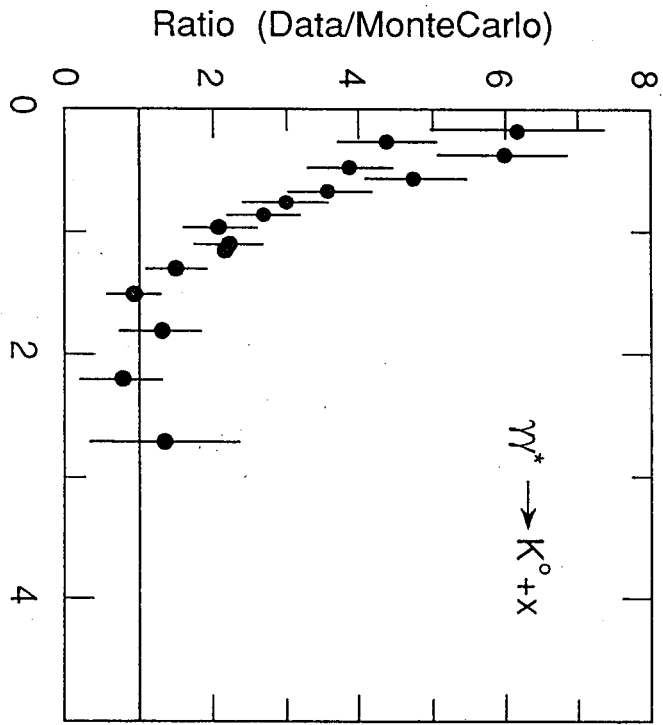
Fig. 2

6-92

P_T (GeV/c)

7176A3

Fig. 3

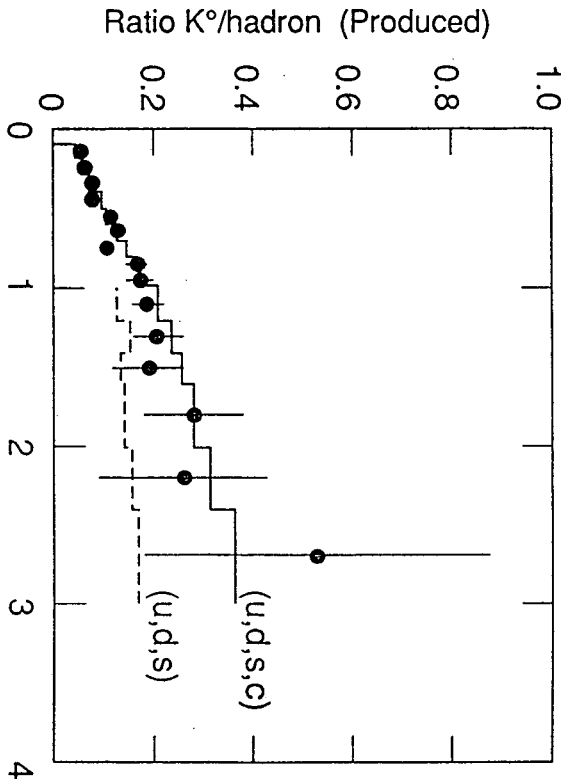


6-92

P_T (GeV/c)

7176A4

Fig. 4



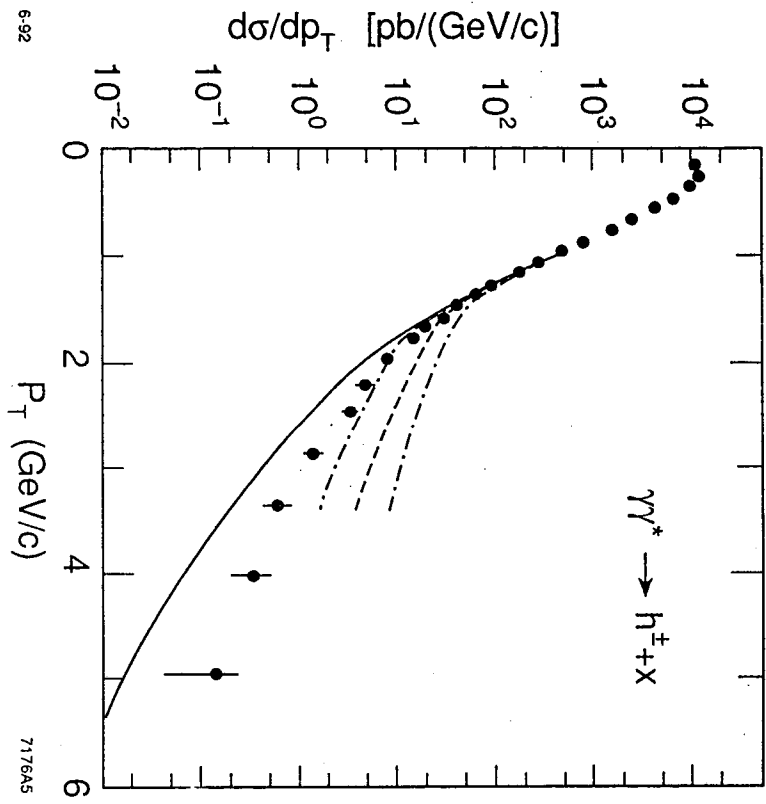


Fig. 5